PHYSICAL REVIEW B VOLUME 16, NUMBER 7 1 OCTOBER 1977

Viscosity and positive-ion mobility near the melting transition in liquid ^{4}He†

F. Scaramuzzi,* A. Savoia,* D.L. Goodstein,‡ and M. W. Cole§
Laboratori Nazionali del Comitato Nazinali per l'Energia Nucleare, Frascati-Roma, Italy,
California Institute of Technology, Pasadena, California 91125,
and Physics Department, Pennsylvania State University, University Park, Pennsylvania 16802
(Received 6 May 1977)

New measurements are presented of the shear viscosity η and the positive-ion mobility μ near the melting transition in liquid ^{4}He. Interpreted in terms of the Stokes law for the drag on a sphere in a viscous medium, it is found, contrary to expectation, that the effective radius of the ion remains constant or decreases slightly as the melting transition is approached at constant temperature. Attempts to explain this observation have not been successful. On the other hand, an older mystery concerning the effective radius of the ion is cleared up: Ahlers and Gamota, comparing data for η and μ at the vapor pressure curve found that the effective radius has a maximum 40 mK below the λ transition (i.e., the lower triple point). We have observed a similar maximum on the melting curve, 40 mK below the upper triple point. It is shown that these maxima may be accounted for by an electrostrictively induced λ transition around the ion. In this interpretation, the maximum along the melting curve serves as the first empirical evidence that the λ line extends into the region of supercooled liquid at pressures above the melting curve.

I. INTRODUCTION

The study of the mobility of ions has long been an important and popular tool for understanding the behavior of liquid helium. Over the years a generally successful picture has emerged, both of the structure of the ions themselves, and of the processes that govern their mobilities, based on experimental data which are most abundantly available at saturated vapor pressure. More recently, in connection with studies of the λ transition, sensitive new techniques have been developed for measuring changes in the mobility,[1] and, in a related quantity, the shear viscosity.[2] In this paper we wish to report a series of experiments designed to apply some of these developments in the vicinity of the melting transition in liquid ^{4}He. In particular we will report new measurements of both shear viscosity and positive-ion mobilities in liquid helium along and near the melting curve in the temperature range approximately 1.7–1.95 K.

Neither the viscosity nor the mobility has previously been explored in detail in this range of temperature and pressure.[3] Moreover, they have not been measured in the same laboratory with comparable sensitivity at any temperature and pressure. It is hoped that these new results may facilitate discussion of a number of questions of general interest, particularly relating to matters such as the nucleation of solidification, the liquid-solid surface tension, and perhaps the existence of a microscopic solid.

In the range of temperatures and pressures we have investigated, the behavior of an ion is generally expected to be hydrodynamic. That is to say, the ion mobility μ and the shear viscosity η may be combined to give an effective radius of the ion, $R_{\rm eff}$, via the Stokes law for the drag on a sphere,

$$R_{\rm eff} = e/6\pi\eta\mu . \tag{1}$$

As we shall see, the identification of $R_{\rm eff}$ with the real radius of the ion may be called into question, but Eq. (1), first suggested by Ahlers and Gamota,[4] can still be regarded as a useful definition.

The ion itself is thought to be a sphere of solid helium formed by the effects of electrostriction.[5] The radius of the sphere, as we shall see in more detail in Sec. III, depends on the applied pressure. As the applied pressure approaches the melting pressure, the radius becomes increasingly sensitive to the liquid-solid surface tension σ. The experiments reported in this paper were originally motivated by the hope that the results would yield a dependable value for σ, a quantity which does not seem to be measurable in any other way. In particular, identifying $R_{\rm eff}$ with the real radius of the ion, σ could be deduced from the rate at which $R_{\rm eff}$ increases as the melting pressure is approached from below.

Having measured $R_{\rm eff}$ along four isotherms approaching the melting curve from below, we found to our considerable surprise that $R_{\rm eff}$ does not increase at all, but rather remains constant or decreases in all cases. As discussed in Sec. IV, we have not found a satisfactory explanation of this observation.

In addition to the measurements along isotherms, we have made measurements along the melting curve. A particularly interesting result of these data is that at about 0.040 K below the λ point (i.e., the upper triple point), $R_{\rm eff}$ undergoes a rather sharp maximum. Ahlers and Gamota[4] have re-

ported the same behavior for R_{eff} along the vapor-pressure curve. In this case, we are able to provide an explanation. The result is what we believe to be the first empirical evidence that the λ line extends into the region of supercooled liquid above the pressure of the melting curve.

Experimental details are discussed in Sec. II. The data and the central ideas behind this work are presented in Sec. III. A summary, including our unsuccessful attempts to explain the behavior of R_{eff} along the isotherms, will be found in Sec. IV.

II. EXPERIMENTAL DETAILS

Measurements of both the viscosity η and the positive-ion mobility μ in the liquid were made along the melting line in the temperature range approximately 1.7 to 1.95 K, corresponding to melting pressures from about 28 to 36 atm. In addition, each quantity was measured along four isotherms, approaching the melting curve from below at temperatures of approximately 1.7, 1.8, 1.9, and 1.95 K. Since the upper triple point occurs at 1.7633 K and 29.741 atm, these data span the λ transition (Fig. 1).

A. Temperature and pressure control

The general apparatus is an improved version of that described in Ref. 1, hereafter called GSS. Its sketch is shown in Fig. 2. It consists of a double-cell system: a main body A, made out of oxygen-free high-conductivity copper, assures good thermal contact between the two cells. Stainless-steel flanges B, fastened to A by indium O-rings, allow gas and electrical connections to the two cells. The upper cell C contains liquid helium in equilibrium with its vapor and acts as the thermoregulating element of the system, with the help of the pumping line D and the thermoregulator elements E (germanium thermometer) and F (heater). The lower cell G contains liquid helium at the same temperature as cell C and at the desired pressure: feed of the gas and pressure control are performed through capillary H. The measuring device, located in cell G, can be either the mobility-measuring diode or the viscosity-measuring vibrating wire system. The two techniques will be described below. The temperature in cell G is monitored by the germanium thermometer I.

The whole system is held in a vacuum can J, evacuated through K, and everything is immersed in the liquid-helium bath L. Depending on the temperature stability requirements in the experimental space (G), this bath can be held at 4.2 K or thermoregulated at a temperature close to the experimental temperature. Under the best conditions (the latter), the temperature within the cell G is kept constant to better than 10^{-5} K.

The pressure is monitored by a Bourdon pressure gauge,[6] with which it is possible to detect the pressure and keep it constant within $\delta P/P \approx 2 \times 10^{-5}$.

With this apparatus it is possible to reach any point in the P, T plane at temperatures from ~1.2 up to 2.17 K and pressures up to the melting curve with the quoted accuracies.

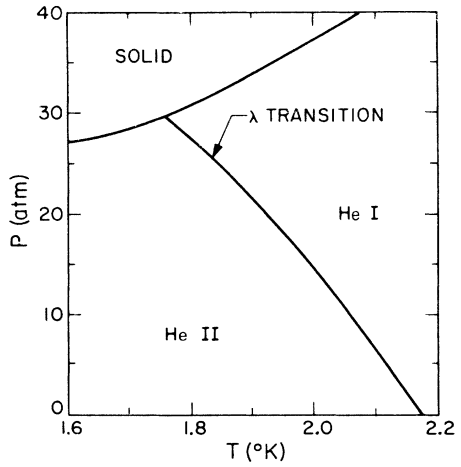

FIG. 1. Phase diagram of ^{4}He in the vicinity of the upper triple point.

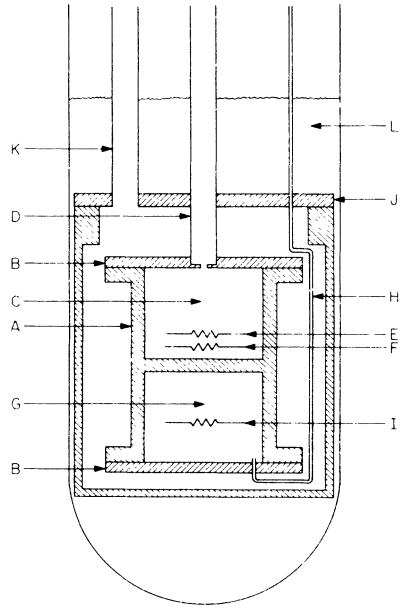

FIG. 2. Schematic diagram of the experimental apparatus. See text for details.

B. Working on the melting curve

Starting from a point close to (below) the melting curve, at constant temperature, a small flow of gas is admitted into cell G (some 10^{-4} mole/sec), causing the pressure to increase slowly and linearly with time. In Fig. 3 the display on a strip-chart recorder of the pressure-gauge output is shown. When the melting pressure is reached, solidification begins and the pressure stops increasing (A). A certain time is allowed in order to be sure that a finite (though small) quantity of solid is formed. Then the gas flow is stopped (B): the pressure undergoes a very small decrease, due to the nulling of the pressure gradient between gauge and cell that occurs when gas is flowing. The pressure after (B) is the melting pressure. The example shown in Fig. 3 occurred in a run at $T = 1.7$ K, i.e., the liquid is superfluid. For runs above the (upper) λ point, due to the finite thermal conductivity of the liquid, the gas flow introduces thermal transients which smooth out the steps shown in Fig. 3. Nonetheless, the melting pressure is equally well determined.

When working along the melting curve, measurements are normally started at the highest temperature. Then, by simply decreasing the temperature without admitting or releasing gas, the system is forced to follow the melting curve.

C. Measurement of the mobility of positive ions

The method used to measure the mobilities of positive ions has been described in detail in GSS.[1] Here only a very short outline of it is given.

A diode, consisting of two plane parallel electrodes contains the liquid helium under investigation. α particles from a ^{210}Po source painted upon one of the electrodes ionize a very thin layer of the liquid. An electric field draws to the other electrode ions of the desired sign, and a current i is measured. If the source is strong enough, complete shielding of the electric field at the source electrode is obtained (full space-charge limitation). In this case, a simple relation between the applied potential V and the ion current i holds[7]: $i = \alpha V^2$. α is proportional to the ion mobility through a geometrical factor. Thus, the measurement of the i, V^2 characteristics of the diode gives the value of the mobility.

In GSS a differential method is described which was devised to yield high resolution. It consists in performing the measurements at constant current i_0 while using a vibrating reed electrometer as a zero meter, by sending into it a signal which nulls the current i_0.[8] The sensitivity of the electrometer can then be increased by a factor of up to 100. In this condition, the value of the applied voltage V is a relative measurement of the mobility ($\mu = \beta V^{-2}$, β being a geometric constant). If the mobility changes, say to μ', a new value of the voltage V' will be required in order to null again the current i_0: then $\mu' = \beta V'^{-2}$. With this method changes in mobility with a resolution up to $\delta\mu/\mu \approx 10^{-4}$ have been measured.

The mobility measurements reported here have been performed with the latter differential technique. Thus they had to be normalized at some point to calibrate the geometry of the measuring cell. The absolute values of μ reported in this paper have been chosen so that on the melting curve at 30 atm, $\mu = 1.44 \times 10^{-2}$ cm^2/V sec. With this choice the values are in agreement with those reported in GSS. Those data in turn had been normalized to agree with a point reported by Ahlers and Gamota,[4] arising from a time-of-flight measurement at the saturated vapor pressure.

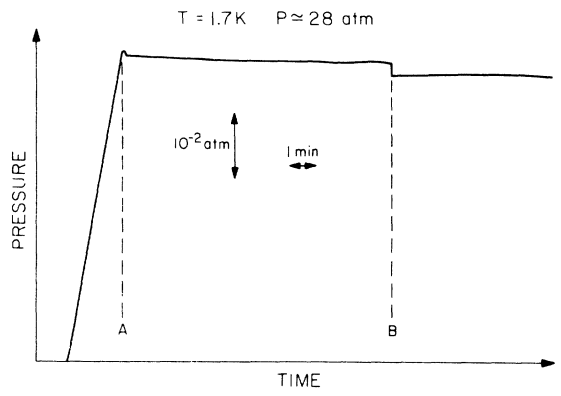

FIG. 3. Chart recorder trace of pressure vs time showing how the melting transition is identified, as discussed in the text.

D. Measurement of the viscosity

The technique used for the viscosity measurements is that devised by Bruschi and Santini to measure the viscosity of liquid ^{4}He near the λ transition, along the vapor-pressure curve.[2,9] Here only the main features of it will be given. For a more detailed description the reader is referred to Ref. 9.

The idea is based on a technique introduced by Tough, McCormick, and Dash.[10] A taut tungsten wire in a transverse magnetic field is caused to vibrate by passing an electric current through it. The damping of the vibrations is dominated by the hydrodynamic parameters of the fluid in which it is immersed. In particular the product of the viscosity and the density ($\eta\rho$) can be determined.

The original technique (Tough *et al.*) consisted in the study of the decay of the vibration produced by

a short pulse of current in the wire. Continuous-wave methods have been devised since then in which the wire is forced to vibrate by a small sinusoidal current of constant amplitude and the resonance response curve is measured. The method devised by Bruschi and Santini, which uses a feedback circuit to lock onto either the in-phase or ±45° out-of-phase component of the response signal, is the most sophisticated and reliable of these.

In principle, the method should have an absolute precision of about 10^{-3} in $\eta\rho$, and a sensitivity of about 10^{-4} to changes in $\eta\rho$. However, two special problems arose in our case which tended to limit the precision of our results.

The tungsten wire has two fundamental modes of transverse vibration which are degenerate in a first approximation. However, internal strains, accidental asymmetries in clamping the ends of the wire, etc. always lift the degeneracy to some extent. Following Bruschi and Santini, our wire was purposely clamped between flat plates at the ends, with the result that the modes parallel and perpendicular to the plates differed in frequency by about 10 Hz (typically, the resonant frequency was about 2700 Hz and the quality factor Q about 300–1000 in helium). The magnetic field is then carefully oriented so that only one of the two modes is excited. However, the alignment in our apparatus is done at room temperature and deteriorates on cooling. In practice it was found that the secondary mode had about one-fifth the amplitude of the principal mode.

Rather than go through the impossibly tedious process of tracing out the full double-resonance curve for each experimental point, a procedure was developed in which measurements were made only of the principal curve, and corrections were applied based on tracing out the complete double-resonance curve at least once in each run. These corrections amounted only to about 1 or 2% in the viscosity. The mathematical technique for making this correction was kindly worked out for us by Dr. T. J. Sluckin.

Values of $\eta\rho$ for pressures up to about 25 atm have been reported by Goodwin,[11] who used the technique of Tough *et al.* To test the overall functioning of our technique we made measurements designed to reproduce those of Goodwin. On certain days we were unable to reproduce his results, invariably obtaining values of $\eta\rho$ considerably higher than his. With the help of a suggestion by Bruschi and Santini, this problem was eventually traced to impurities in the helium we were using. We have no explanation for how impurities could have caused the result: we estimated that the impurity level could have been no higher than about 50 ppm (given the helium temperature capillaries through which the helium gas was introduced into the cell). However, our values of $\eta\rho$ were higher than Goodwin's by a factor of 2 to 3. Nevertheless, the problem vanished when we adopted a procedure in which the gas to be condensed for measurement of viscosity was first passed slowly under pressure through a liquid-nitrogen-cooled zeolite trap, and considerable care was taken after condensation that no contaminants were introduced subsequently into the measurement cell. With these precautions we could always reproduce Goodwin's results within his stated uncertainty of a few percent, and that check was made in the course of each run from which data are reported in this paper.

As stated above, the measurements yield essentially the product $\eta\rho$. Above the λ transition small variations in the density with temperature and pressure were obtained from a smooth functional fit to the equation of state,[12] so that η could be extracted. Below the λ transition, however, ρ_n has to be taken into account rather than ρ, and this quantity varies much more rapidly. There were no independent measurements of ρ_n available in the region of P and T of interest. Thus, an interpolation procedure for ρ_n had to be adopted in order to deduce η.

Romer and Duffy[13] have reported values of ρ_n/ρ along isobars, at roughly 5 atm intervals up to 25 atm. In addition Ahlers[14] has given a universal formula for the limiting dependence of $\rho_s/\rho = 1 - \rho_n/\rho$ as the λ line is approached at any temperature and pressure. By extrapolating the λ line to pressures above the melting curve and assuming that Ahlers' formula continues to be valid, it was possible to construct plots of ρ_n/ρ vs pressure for a series of constant temperatures. Smooth curves were drawn which passed through the points reported by Romer and Duffy and had the limiting slope required by Ahlers. Since the region of interest for our data fell between the limits of the Romer and Duffy data and Ahlers' formula, this procedure resulted in values of ρ_n/ρ that were interpolated rather than extrapolated from either side. A finer grid of interpolations along isobars between these isotherms was finally constructed in order to find ρ_n/ρ at the precise values of P and T where our data lie.

It is difficult to estimate the uncertainties introduced by this procedure. They include extrapolation of the λ line (assuming constant slope) into the region of supercooled liquid, the use in this region of Ahlers' formula which is essentially a fit to data at lower pressures designed to conform to the assumption of universality in critical phenomena, and finally, an interpolation between data arising from different laboratories. On the other hand, smooth

interpolation curves were remarkably easy to draw between these data, so that a table of values of ρ_n/ρ with three significant figures could be constructed with some confidence. Moreover, the corrections by interpolation are not very large. Typically, each value of ρ_n/ρ finally used falls within 10% of the nearest measured value of Romer and Duffy; thus a substantial error in the 10% interpolation still introduces an absolute error in η of order of the other uncertainties in the vibrating-wire linewidth measurements themselves. The relative values of η are affected even less. For example, along the viscosity isotherm at 1.690 K, ρ_n/ρ was found to vary by only about 7% over the pressure range studied.

Taking into account all of the difficulties outlined above, including the uncertainties introduced by the evaluation of ρ_n/ρ below the λ transition and by possible thermal problems above the transition, we estimate the possible error in the reported absolute values of the viscosity to be roughly 2%, and in the relative values about 0.2% or less.

In the mobility measurements, the errors are, respectively, about half as large. These estimates are in good agreement with the observed reproducibility of the results.

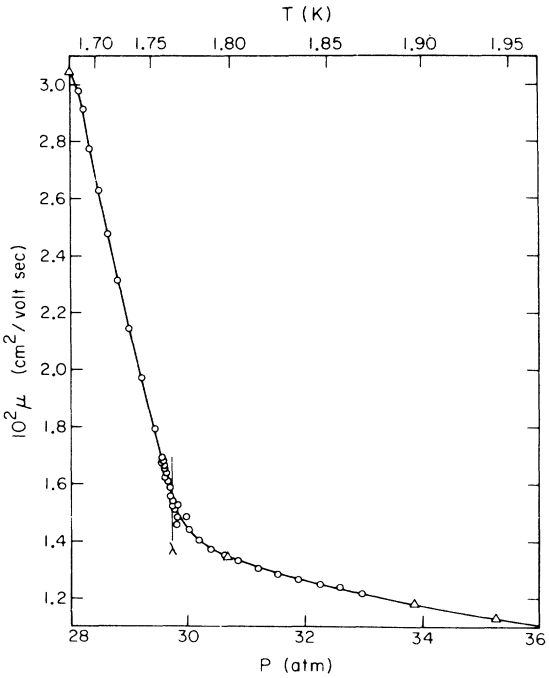

FIG. 4. Positive ion mobility vs pressure (lower scale) or temperature (upper scale) along the melting curve. Circles: points taken while following the melting curve, as described in Sec. II of the text. Triangles: end points of isotherms shown in Fig. 9 below.

III. DATA AND DISCUSSION

Absolute values of the positive-ion mobility along the melting curve are plotted in Fig. 4. Relative changes in μ along isotherms are plotted as open circles in Fig. 9 below.

Data for the viscosity along the melting curve together with the values of ρ_n/ρ that were used are tabulated in Table I, and the viscosity is plotted in Fig. 5. Relative values of viscosity along the isotherms are shown in Fig. 9 and tabulated in Table II, together with the values of ρ_n/ρ used in deducing them.

A. Viscosity

All of the viscosity data above the λ transition, both melting curve and isotherm data, are plotted vs pressure alone in Fig. 6. At high pressures, all of these data are seen to fall on a single curve, implying that the viscosity in this region is independent of temperature, depending only on pressure. Over the limited range studied, these data are well fitted by a straight line shown in the figure,

$$\eta_0(P) = 2.98P - 10.5 \qquad (2)$$

where η_0 is expressed in μP and P in atm. Below approximately 33 atm, the melting data depart from this behavior, but the isotherm data continue to follow it. Moreover, the isotherm data at 1.8 K depart from the melting data, running more nearly parallel to the line followed at higher P.

There is a simple interpretation to these observations. In the region under study, a given decrease in pressure along the melting curve brings the system much closer to the λ transition than would the same decrease in pressure along an isotherm (see Fig. 1). Thus the data suggest that the viscosity in this region consists of two parts: an underlying temperature-independent component given by Eq. (2), and a second part which is a consequence of approaching the λ transition. To test this interpretation, we use as a measure of the distance from the transition a reduced temperature t given by

$$t = [T - T_\lambda(P)]/T_\lambda(P)\,, \qquad (3)$$

where the λ temperature at pressure P, $T_\lambda(P)$, is found by extrapolation of the λ line mentioned above when P is greater than the pressure of the upper triple point. If the interpretation we are pursuing is correct, then the difference between the measured values, η, and the values $\eta_0(P)$ given by Eq. (2) should be a universal function of t. Figure 7 is a plot of $\eta^* = \eta_0(P) - \eta$ vs t, showing that η^* is indeed a function of t alone.

A recent theory by Goodstein[15] of the viscosity

TABLE I. Data for the viscosity η along the melting curve, together with the values of ρ_n/ρ that were used. The values of the end points of the four isotherms are also reported.

T(K)	P(atm)	$\eta(\mu P)$	ρ_n/ρ
1.690	28.19	31.30	0.614
1.690	28.19	30.81	0.614
1.704	28.44	33.88	0.659
1.721	28.77	37.32	0.751
1.739	29.16	47.14	0.802
1.739	29.16	47.60	0.802
1.759	29.65	64.30	0.936
1.759	29.65	64.37	0.936
1.779	30.19	73.60	
1.798	30.74	77.91	
1.816	31.26	80.92	
1.835	31.82	83.64	
1.835	31.82	84.07	
1.835	31.82	82.61	
1.853	32.41	85.14	
1.871	32.97	87.36	
1.903	34.00	91.06	
1.925	34.73	93.22	
1.940	35.26	94.60	
[a]1.690	28.19	31.52	0.614
[a]1.799	30.74	75.07	
[a]1.902	33.97	91.48	
[a]1.948	35.94	95.47	

[a] End points of the isotherms.

TABLE II. Relative values of viscosity $(\eta_m - \eta)/\eta$ (η_m is the value of the viscosity at the melting curve) as a function of the pressure P along isotherms in the vicinity of the melting curve. The values of ρ_n/ρ that were used are also reported.

	P(atm)	$(\eta_m - \eta)/\eta$	ρ_n/ρ	
$T = 1.690$ K	26.80	0.1237	0.575	
	27.03	0.1060	0.581	
	27.26	0.0835	0.587	
	27.49	0.0696	0.594	
	27.72	0.0451	0.601	
	27.96	0.0244	0.608	
	28.19	0	0.614	melting
$T = 1.799$ K	29.36	0.0812		
	29.36	0.0644		
	29.83	0.0516		
	30.07	0.0377		
	30.30	0.0242		
	30.52	0.0120		
	30.74	0		melting
$T = 1.902$ K	30.92	0.1186		
	32.58	0.0549		
	32.85	0.0475		
	33.14	0.0343		
	33.44	0.0225		
	33.75	0.0166		
	33.97	0		melting
$T = 1.948$ K	34.32	0.0420		
	35.56	0.0336		
	34.80	0.0240		
	35.03	0.0159		
	35.26	0.0092		
	35.49	0		melting

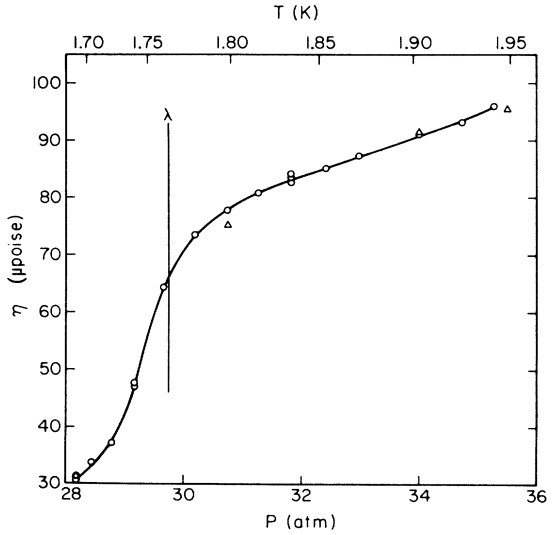

FIG. 5. Viscosity vs pressure (lower scale) or temperature (upper scale) along the melting curve. Circles: points taken while following the melting curve, as described in Sec. II of the text. Triangles: end points of isotherms shown in Fig. 9 below.

of helium near the λ transition suggests that the viscosity above the transition should divide in just this way, into a part representing the behavior of normal fluid far from the transition, and a (negative) contribution owing to approaching critical behavior. In particular, in this view, the negative contribution, or η^*, is proportional to the volume fraction of the liquid, which at any instant has undergone a fluctuation into an isolated region of superfluid, whose characteristic dimension is of order of the correlation length ξ. Thus, η^* would be proportional to the fraction of the fluid which is superfluid by fluctuation. An earlier work by Ferrell *et al.*,[16] similarly describes spatial variation of the superfluid properties. This work yields an estimate of the superfluid density at fixed finite wave number above the transition which has the same characteristic convex downward shape shown by η^* in Fig. 7.

These comments are, of course, no more than suggestive. However, it should be worthwhile to obtain further viscosity data at lower pressures

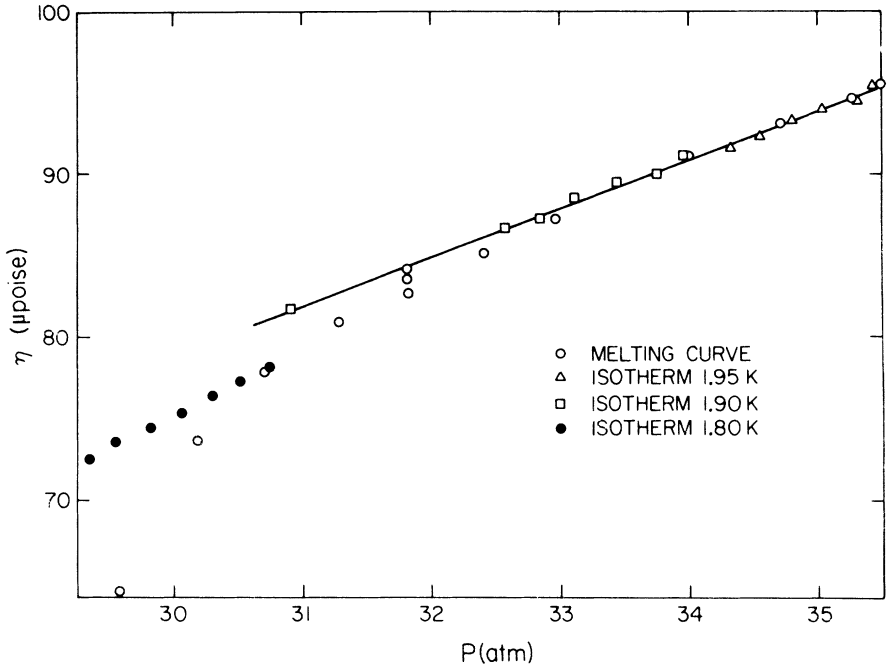

FIG. 6. Viscosity vs pressure above the lambda transition showing points both along isotherms and along the melting curve. The straight line follows Eq. (2) of the text.

in the range roughly $0.01 < t < 0.1$ to see if these observations continue to hold.

B. Mobility

The original motivation for the work reported in this paper was the possibility of extracting the liquid-solid surface tension of helium, σ, from measurements of the positive-ion mobility near melting. The positive ion in liquid helium may be thought of as an unshielded charge in a dielectric medium. The electric field of the ion polarizes helium atoms, then attracts the resulting dipoles. There is thus an attractive force on the medium arising from a potential which varies as the square of the electric field. The simplest approximation takes the liquid to be incompressible, in which case the pressure p_l at distance r from the ion exceeds the applied pressure P by a function

$$p_l - P = \beta / v_l r^4 , \tag{4}$$

where β depends on the polarizability of helium, and v_l is the molar volume. At some distance, say R_m, from the ion, p_l becomes equal to P_m, the melting pressure of helium at the bath temperature. If the helium became solid at that point, we could imagine the ion surrounded by a self-induced sphere of solid, whose radius according to Eq. (4) would grow to infinity as P approached P_m.

For temperatures in the vicinity of T_λ and above, the mobility, the viscosity, and the radius associated with the ion should be related by Eq. (1) arising from Stokes' drag. If, as argued above, $R_{\text{eff}} = R_m \to \infty$ as $P \to P_m$, then we should observe $\mu \to 0$ as the pressure in the bath approaches the melting curve. However, before these investigations began, it was well known that μ did not go to zero as the melting curve is approached.[4,17]

The reason R_{eff} does not go to infinity as melting is approached depends on the existence of a solid-liquid surface tension at the interface between the solid sphere induced about the ion and the liquid medium. If we compress a bulk solid and liquid in equilibrium with a planar interface, the volume of solid can grow at constant pressure without any increase in interfacial area. However, the spherical solid around the ion cannot grow without in-

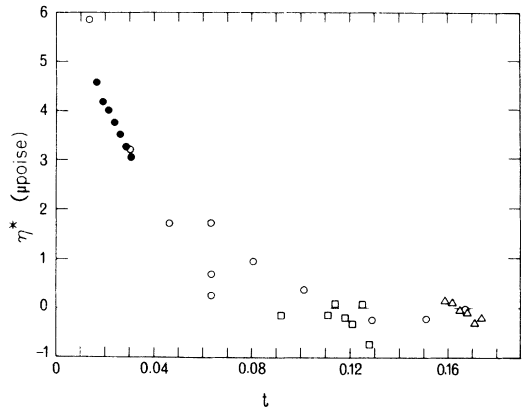

FIG. 7. The excess viscosity, $\eta^* = \eta_0(P) - \eta$ as explained in the text, vs reduced temperature as defined in Eq. (3). Symbols are the same as those in Fig. 6.

TABLE III. Definitions of radii used in the text.

r,	distance from the center of the ion core.
R_{eff},	Stokes or hydrodynamic radius, defined in Eq. (1).
R_s,	radius of solid sphere presumed to be induced about the ion by electrostriction.
R_λ,	radius of the sphere of normal fluid induced about the ion by electrostriction.
R_0,	characteristic distance derived from parameters of the fluid. Defined by Eq. (13).
R_m,	distance from ion core at which the bulk melting pressure is reached.

creasing its surface area. Since there is a positive surface tension, or free energy per unit area of interface, there is a higher cost in free energy to increase the volume of the sphere than to increase the volume of the bulk solid. The result is that the local pressure at which the helium solidifies is higher than the bulk melting pressure P_m, and the ion is then surrounded in the region between the solid and R_m by supercooled but stable liquid. Conversely, as the applied pressure approaches P_m, R_{eff} remains finite.

These considerations are easily expressed thermodynamically. To avoid confusion with the mobility, let us use the symbols $g_l(P)$ and $g_s(P)$ for the chemical potentials of the liquid and solid, respectively, at pressure P (the temperature will be assumed constant). We also introduce the symbol R_s for the radius of the solid, recognizing that it may not be equal to the hydrodynamic radius R_{eff} defined in Eq. (1). (As an aid to the reader, we present in Table III, a list of the various radii used in this paper.) If the pressure in the liquid at the interface of the sphere is P_l, then the pressure in the solid is $P_l + 2\sigma/R_s$. Thus,

$$g_s(P_l + 2\sigma/R_s) = g_l(P_l) . \tag{5}$$

We also know that $g_l - \beta/r^4$ is uniform from $r = R_s$ to $r = \infty$:

$$g_l(P) = g_l(P_l) - \beta/R_s^4 . \tag{6}$$

We can refer these chemical potentials to the bulk melting pressure, where

$$g_s(P_m) = g_l(P_m) . \tag{7}$$

Using the identity $(\partial g/\partial P)_T = v$ and appropriate equations of state, these equations can be used to find R_s as a function of P. If for simplicity we assume incompressibility of both liquid and solid, we find

$$P_m - P = \frac{\beta}{v_l R_s^4} - \frac{2\sigma}{R_s}\,\frac{v_s}{v_l - v_s} , \tag{8}$$

where v_s is the molar volume of the solid. This entire argument was originally put forth by Atkins.[5]

Thus, although R_s does not diverge, it does increase as P is increased towards P_m and its magnitude is governed by σ,[17] especially near P_m. Therefore, a measurement of how R_s depends on P near melting would afford a sensitive means of measuring σ. The solid-liquid equilibrium surface tension is a quantity of fundamental importance, which has never been measured in any substance by any other means.

The idea, then, was to measure the mobility, use the result to find $R_s(P)$, and therefore deduce the surface tension. The sensitive differential technique, developed for measuring the critical behavior of μ near the λ transition would be applied near the melting transition where R_s varies most rapidly, and depends most sensitively on σ. If we assume $R_s = R_{eff}$, we may substitute Eq. (1) into Eq. (8) yielding a dependence of μ on P (at constant T) of the form

$$P_m - P = a\mu^4 - b\mu , \tag{9}$$

where a and b will be constants if the variation of η with P may be neglected. If these arguments are correct, and the approximations we have made are reasonably good, a plot of $(P_m - P)/\mu$ vs μ^3 should be a straight line whose slope and inter-

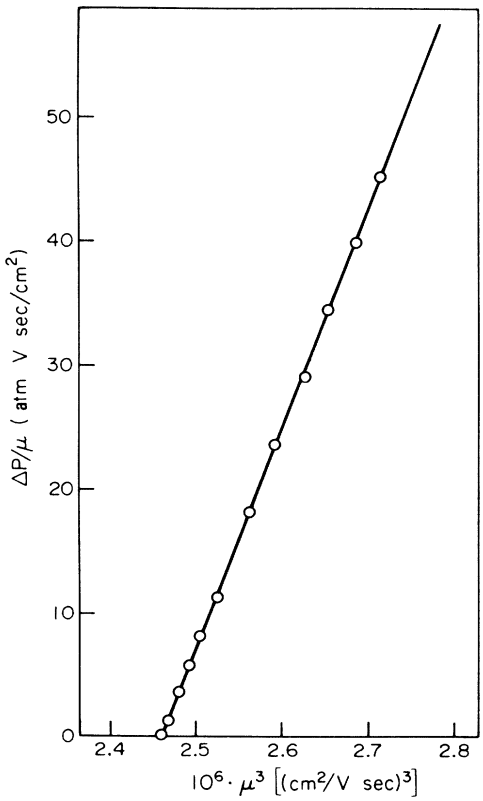

FIG. 8. Plot of $(P_m - P)/\mu^3$ for an isotherm approaching melting at 1.71 K.

cept would yield the viscosity near melting (not then yet measured) and σ.

Accordingly, mobilities along isotherms near melting were measured, and the required plots were made.[18] An example, from data at 1.71 K, is shown in Fig. 8. Excellent straight lines were obtained, and values of η and σ deduced. In the case illustrated, the results were $\eta = 45.4$ μP and $\sigma = 3.04 \times 10^{-2}$ ergs/cm^2. The value for η, as we may now see from our own data, Fig. 5, is a bit high, the directly measured value being about 35 μP at melting, but it is of the right order of magnitude. The value of σ seems sensible as well; one would expect it to depend on the difference in density between the phases separated by the interface. The solid-liquid density difference is about 10 times smaller than the liquid-gas density difference, and the deduced value of σ, is, indeed, about 10 times smaller than the known value of the liquid-gas surface tension (approximately 3.7×10^{-1} ergs/cm^2).

Nevertheless, we found it disquieting to observe that σ seemed to change more rapidly with temperature over the narrow range studied than could reasonably be expected. The surface tension appeared to increase from 0.030 ergs/cm^2 at 1.7 K to 0.036 ergs/cm at 1.8 K, and again to 0.041 ergs/cm at 1.9 K. Over the same range, the solid-liquid density difference barely changed, and in fact, decreased slightly. We would have expected σ to remain nearly constant, independent of temperature, over this range.

After carefully repeating the experiments, reanalyzing the data, and reevaluating the theory (including, e.g., the assumption that the liquid and solid are incompressible), it was decided that the principal source of error in this analysis was the assumption that the viscosity did not vary significantly along the isotherms studied. In Eq. (9), the coefficients a and b both depend on the viscosity. If η varies with P, then the dependence of μ on P is due not only to the changes in R_s when P_m is approached, but also to the changes in η. Thus the interpretation of Fig. 8 and the resulting values for σ would be in error. It is also true that R_s might not be equal to the measurable quantity R_{eff}, but we had reason to believe the two might be related by a constant factor.[17]

It was as a consequence of this argument that we installed the instruments for measuring η. The idea was to measure the variation of η with P along the same isotherms that we measured $\mu(P)$. The contribution of the variation of η could then be subtracted from the change in μ and σ extracted from the remainder. This comparison could be done with reasonable accuracy even if each quantity changed by only a few percent per atmosphere, since the techniques for measuring both μ and η are much more sensitive to changes than to absolute values.

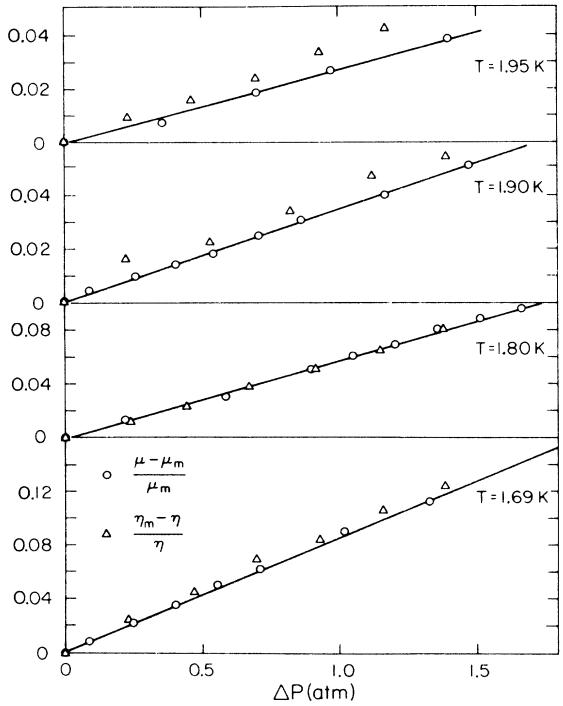

FIG. 9. Changes in μ and η with respect to their values at melting, on isotherms approaching melting. Lines are drawn through mobility data to facilitate comparison with changes in viscosity.

The results of this program are shown in Fig. 9. On each of four isotherms, $(\mu - \mu_m)/\mu_m$ (open circles) and $(\eta_m - \eta)/\eta$ (triangles) are plotted versus $P_m - P$. The reason for plotting the data in this way is that $(\mu - \mu_m)/\mu_m - (\eta_m - \eta)/\eta \propto \mu\eta - \mu_m\eta_m \propto R_{eff}^{-1} - R_{eff\,m}^{-1}$, where $R_{eff\,m}$ is the value of R_{eff} at melting. Thus the difference in these curves on each isotherm shows the variation of R_{eff} as melting is approached. It is seen that, contrary to all expectation, $(\mu - \mu_m)/\mu_m \leq (\eta_m - \eta)/\eta$. In other words, interpreting these results in light of Eq. (1), it appears that in all cases R_{eff} *remains constant or decreases* as P approaches P_m. In view of the possible implications of these observations for the long-standing and widely accepted picture of the structure and hydrodynamics of the positive ion, we defer further discussion of this point to Sec. IV.

Although the most surprising feature of these data is the fact that η generally changes more rapidly than μ, it should also be noted that the product $\eta\mu$ really changes very little. We can see from Fig. 9 that R_{eff} changes by no more than about 1% along any of the isotherms studied. To investigate this point further, we have constructed values of R_{eff} along the melting curve in order to see how it

changes with temperature.

The values of R_{eff} could not be constructed directly from the data, since we do not have (η, μ) pairs at the same temperature and pressure on the melting curve. Instead, the smooth curve shown in Fig. 4 was used to find values for μ at the points where η had been measured. The resulting behavior of R_{eff} at melting is shown in Fig. 10.

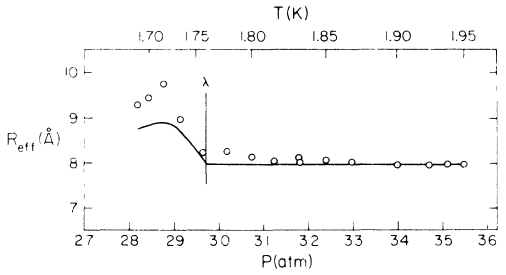

FIG. 10. Effective radius vs pressure (lower scale) or temperature (upper scale) along the melting curve. Solid curve is the prediction of the model discussed in the text.

Far above the λ transition, R_{eff} rises gently as T is decreased. Below the transition, it rises more sharply, passing through a maximum at about 1.72 K, then falls again. Ahlers and Gamota,[4] studying R_{eff} along the ^{4}He vapor-pressure curve, have also noted a maximum about 40 mK below the transition. They suggest that the phenomenon may be due to electrostriction,[19] but express doubt that the 40-mK displacement can be accounted for quantitatively on that basis. We wish to present a model which shows how it may be done.

The model applies anywhere along the λ line. For simplicity we will discuss its application to our own data at melting. Imagine the liquid to be near the melting curve, below the λ point, and once again consider the effect of electrostriction. The radius of the solid sphere is not very important for this argument, so we shall take it to be constant (equal to 7.95 Å). At some distance R_λ from the ion, the rising pressure induced by the ion passes through the extrapolation of the λ line into the supercooled liquid as sketched in Fig. 11. Thus, two phase transitions occur as we move outward from the ion: at R_s the solid changes to liquid, then at R_λ the normal liquid changes to superfluid. R_λ is given by the value of r in Eq. (4) when p_l is equal to the extrapolated λ pressure, P_λ.

The viscosity of the fluid surrounding the ion depends on pressure (as we may see from our own data) and therefore varies continuously with distance from the ion core. However, to understand qualitatively how the mobility of the ion may be expected to behave, it is sufficient to simplify the picture.

Since the viscosity changes rapidly in the vicinity of R_λ, and relatively slowly elsewhere, we can take the ion to be surrounded from R_s to R_λ with fluid of viscosity η_n, a value characteristic of the normal fluid above the λ transition, and between R_λ and infinity by fluid of the measured viscosity η. Now let us imagine qualitatively, the behavior of the quantity R_{eff} deduced from measurements of μ and η and plotted in Fig. 10. At the λ transition and above, R_λ is infinite, so the core is surrounded to infinity by fluid of viscosity η_n. However η_n is also the value measured by the vibrating wire. R_{eff} is therefore just equal to the core radius, 7.95 Å. On the other hand, below the transition, as $P_\lambda(T)$ increases, R_λ becomes small, eventually becoming equal to the core radius. At that point, the sphere is surrounded to infinity by fluid of viscosity η, which is once again the value measured by the vibrating wire. Thus at both of these extremes, $R_\lambda = \infty$ and $R_\lambda = R_s$, R_{eff} is just equal to the core radius $R_s = 7.95$ Å.

However, between these extremes, the core is surrounded out to a finite radius R_λ by a fluid whose viscosity is larger than the measured value. Consequently, the mobility is lower than one would expect on the basis of the measured viscosity. R_{eff} as defined in Eq. (1) is therefore larger than the core radius. Since R_{eff} is equal to the core radius at both extremes and larger in the middle, it follows that it must have a maximum. We believe this to be the explanation of the observed behavior.

The arguments we have given may be made somewhat more quantitative using a result presented by Goodstein.[15] He has calculated the drag on a sphere for precisely the model we have proposed, the core surrounded by a self-induced sphere of different viscosity from that further away. The result for

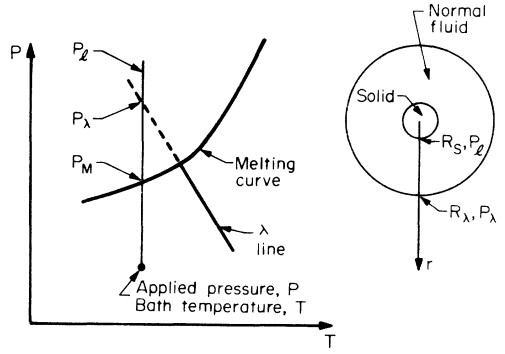

FIG. 11. Sketch illustrating the effects of electrostriction induced by a positive ion in ^{4}He below the λ line. Left: schematic of the pressure-temperature plane including extrapolation of the λ line into the super-cooled region. Right: sketch of the ion.

R_{eff} as we define it in Eq. (1) is

$$R_{eff} = \tfrac{4}{3} q R_s A , \tag{10}$$

where $q = \eta_n/\eta$ and

$$A^{-1} = \frac{4}{3}\frac{R+q-1}{R} + \frac{10}{3}\frac{(R^2-1)^2(q-1)}{R^5(3q+2)+2(q-1)} , \tag{11}$$

where $R = R_\lambda/R_s$. To use this result in the simplest possible way, we have calculated R_{eff} along the melting curve, taking $\eta_n = \eta$ (the measured value) above the λ transition, and η_n fixed at η_λ below the transition (η_λ is the measured viscosity at the transition). R_s is assumed constant, R_λ due to electrostriction is calculated at each point, and measured values of η are used. The result is shown as a solid curve in Fig. 10. Above the transition, $R_\lambda = \infty, q = 1$, $A = \frac{3}{4}$, so $R_{eff} = R_s$. Below the transition, the expected maximum in R_{eff} is clearly seen, occurring just where the experimental maximum is observed.

Various quantitative refinements of the model are possible. For example, instead of the choice made above for η_n, we could use the values given by Eq. (2), taking η_n to be equal to $\eta_0(P)$. In that case, the rise in R_{eff} as the transition is approached from above is produced by the model (since q is no longer constant above the transition), and the maximum in R_{eff} below the transition is also produced, once again in the same position. However, the quantitative assumptions (e.g., ignoring variations in the density of the fluid, variations in the viscosity within each region, and so on) are not meant to be convincing in detail, and we do not expect to be able to fit the data with a theoretical curve. The simpler model plotted in Fig. 10 serves to illustrate that the qualitative behavior is understood in principle. In particular, we believe the maximum in R_{eff} observed both at the vapor pressure and at the melting curve, is due to an electrostrictively induced λ transition around the ion. Thus, the maximum shown in Fig. 10 along the melting curve is clear evidence that the λ line may be extrapolated through the melting curve into the region of supercooled liquid.

If the solidification of helium could be retarded, and the supercooled liquid studied, it certainly seems reasonable to believe that the λ line would be observed to continue into this region. To our knowledge, however, the maximum in Fig. 10 is the first empirical evidence that it actually does so. It has been possible to obtain this empirical evidence because the supercooled liquid is in fact thermodynamically stable in the vicinity of a positive ion, and its properties thus influence the behavior of positive ions.

IV. ANOMALOUS PRESSURE DEPENDENCE NEAR MELTING

The principal dilemma presented in this paper is the fact that close to the melting curve the mobility of positive ions varies less rapidly with pressure than does the shear viscosity. This observation is surprising when viewed in the context of macroscopic thermodynamics and continuum hydrodynamics where the two measurements are related to each other by means of Atkins' "snowball" model of the ion and Stokes' law for the drag on a sphere. This approach has in the past enjoyed considerable success, and so we shall in this section discuss whether reasonable modifications of the theories involved can help to account for our observations.

The problem can be divided into two parts: the structure of the solid sphere on the one hand, and the hydrodynamics on the other. Let us consider them separately. What we need to explain is why the effective radius of the sphere as defined in Eq. (1) decreases with increasing pressure along isotherms approaching the melting curve (see Fig. 9).

In spite of a number of uncertainties, it is difficult to imagine any sensible model in which the actual radius of the sphere, R_s, decreases when the pressure is increased. We have already seen that for an incompressible fluid, R_s always increases with increasing pressure. Better quantitative predictions can be made by using more realistic equations of state for both liquid and solid, and also by including other effects such as the potential acting in the fluid due to the enhanced density of the solid.[20] In all of these cases, the liquid-solid surface tension σ enters as a parameter, but is assumed to be constant, independent of R_s. In all cases, regardless of the choice of σ, R_s increases with increasing applied pressure.

One could reasonably imagine that for these very small spheres (typically $R_s \sim 5$ to 7 Å) σ should be taken to vary with R_s. In particular we would expect σ to decrease towards its flat interface value as R_s increases on the basis of a simple model describing atomic interactions at the interface. This decrease in σ only causes R_s to increase even more rapidly with increasing applied pressure than one would predict with the assumption of constant σ.

We conclude, therefore, that the answer to our dilemma will not be found in any thermodynamic analysis of the behavior of the radius of the sphere.

It is possible, of course, that a solid sphere, in the sense of an interface at which the density is nearly discontinuous, never forms at all. If no solid forms, one must imagine a continuous variation of η and ρ in the fluid surrounding the ion.

One cannot know with confidence the associated μ, but it is at least possible that μ would change less rapidly than the measured viscosity. However, since we cannot be certain the extreme step of discarding the snowball model would help to explain our observation, we turn now to a discussion of the hydrodynamic problem, retaining the picture of a solid sphere formed about the ion.

The hydrodynamic problem is to modify the Stokes solution of the Navier-Stokes equations to take into account the fact that owing to electrostriction neither the density nor the viscosity of the fluid are uniform, both increasing as the ion is approached from far away. No general analytic solution to this problem exists, but Ostermeier and Schwarz[17] have given numerical solutions for some special cases, and we shall use their solutions as the starting point of our discussion.

In order to make quantitative use of the Ostermeier-Schwarz solutions (or any other solutions) it is necessary to know how, e.g., the viscosity varies with distance from the ion, $\eta(r)$. At sufficiently large distance, the necessary dependence can be deduced from our own data for how η depends on P. However, as we have seen, at small r, the fluid is supercooled (i.e., the pressure P is greater than the melting pressure P_m) and in that region the viscosity is not known and cannot be measured. Although we must therefore use extrapolations, the results, as we shall see, do not seem to be very sensitive to the technique used for extrapolating.

To simplify the analysis, we accept Ostermeier and Schwarz's finding that density variations do not affect the result greatly, and take the density to be constant. Ostermeier and Schwarz parameterize the viscosity variation by the form

$$\eta(r) = \eta_\infty e^{\tau (R_s/r)^m} . \tag{12}$$

Our own measurements of what is here called η_∞ show that it varies with P according to Eq. (2). Moreover, the local pressure p_l is related to the applied pressure by Eq. (4). Letting P in Eq. (4) be called P_∞ to be consistent with the present notation, and substituting p_l in Eq. (4) for P in Eq. (2), we find

$$\eta = \eta_\infty + \left(\frac{\partial \eta_\infty}{\partial P_\infty}\right) T^6 \Big/ v_l r^4 \equiv \eta_\infty \left[1 + \left(\frac{R_0}{r}\right)^4\right] , \tag{13}$$

where $\partial\eta_\infty/\partial P_\infty = 2.98$ μP/atm according to Eq. (2), and $R_0 = [\beta(\partial\eta_\infty/\partial P_\infty)/v_l\eta_0]^{1/4} \simeq 6.5$ Å near melting at 1.95 K. R_0 is a characteristic distance given by properties of the fluid and is not related to any property of the ion. Eq. (12) agrees with Eq. (13) at large r if we choose $m = 4$ and $\tau = (R_0/R_s)^4$. Equation (12) is then a possible extrapolation of the viscosity to the region close to the sphere [Eq. (13) by itself is an alternative extrapolation].

In the solution given by Ostermeier and Schwarz, μ and η are related by Eq. (1), with R_{eff} given by

$$R_{eff} = FR_s , \tag{14}$$

where F depends on the parameters m and τ. With the choice $m = 4$, we find that the results of Ostermeier and Schwarz satisfy

$$F \cong 1 + 0.15\tau , \quad 0 \le \tau \lesssim 2.5 , \tag{15}$$

with F falling below this line for larger values of τ. Together with the identification of τ above, we have

$$R_{eff} = R_s[1 + 0.15(R_0/R_s)^4] . \tag{16}$$

This equation means that if we could increase R_s without changing $\eta(r)$ in the fluid, we would find that R_{eff} has a minimum at $(R_0/R_s)^4 = \tau = 2.2$. For smaller R_s (larger τ), R_{eff} actually decreases as R_s increases; everything else remains constant. Thus this result affords a possible basis for an explanation of the observed decrease of R_{eff} with pressure. However, before pursuing the point it is desirable to have a clearer idea of the physical reasons for this behavior than the numerical calculation affords us.

Fortunately, it is possible to give an analytic derivation of Eq. (15) which does shed light on the physical mechanism involved.[21] Rather than trying to solve the Navier-Stokes equations for the velocity field of the moving ion, we start instead from the expression for the rate of energy dissipation in the fluid,[22]

$$\dot{E} = -\frac{1}{2} \int \eta(r) \left(\frac{\partial v_i}{\partial x_j} + \frac{\partial v_j}{\partial x_i}\right)^2 dV , \tag{17}$$

using the summation convention. Here the volume integral extends over all space and v_i are the components of the velocity field. If the ion drift velocity is u, then the drag force is $-\dot{E}/u$, and the mobility is $-eu^2/\dot{E}$. To find the leading order correction to the standard Stokes problem, we use for the velocity field the well-known Stokes solution for constant viscosity,[23] but for the viscosity, we use the expression given in Eq. (13). Performing the integral indicated in Eq. (17), we find that the mobility once again obeys Eqs. (1) and (14), with

$$F = 1 + \tfrac{47}{315} (R_0/R_s)^4 . \tag{18}$$

Recognizing that $\frac{47}{315} \approx 0.15$, and comparing to Eq. (15), we see that we have reproduced the Ostermeier and Schwarz (OS) solution in this domain. Conversely, from the OS solution, we see that the range of validity of the approximations we have made in this argument is $0 \le (R_0/R_s)^4 \lesssim 2.5$. Notice

that in this domain it apparently does not matter whether we use Eq. (12) or Eq. (13) to extrapolate the viscosity. Thus the uncertainty introduced by extrapolating the viscosity may not be serious.

By examining Eq. (17), we can now see what governs the drag on the ion in the nonuniform fluid. The density of energy dissipation [the integrand of Eq. (17)] depends on both the viscosity and the derivatives of the velocity. In the real fluid, when η becomes large at small r, it tends to damp gradients in the velocity field, keeping the energy dissipation low. That effect is not taken into account in the approximation we have made, which is the reason the result fails at large $(R_0/R_s)^4$. Thus, in this approximation, as R_s grows, it freezes out regions of very high energy dissipation, so that the drag force itself can actually appear to decrease. Even when this solution is valid, however, R_{eff} can decrease as R_s increases. In a realistic solution, the integrand of Eq. (17) goes to zero both at large r and at small r (where the motion is frozen out, either by rising viscosity or by actual freezing of the sphere). Clearly, there is a region of maximum energy dissipation in between, and it is not hard to guess that this must occur around $r = R_0$. Thus, as R_s increases towards R_0, it tends to freeze out regions of relatively high dissipation and this mechanism can actually cause R_{eff} to decrease.

The arguments we have given here tend to indicate that the hydrodynamic solutions at hand are capable of giving a qualitative, and even a fairly good quantitative account of the observations under discussion. Accordingly, we have tried to fit the data using the following analysis: using the best available data for the liquid and solid equations of state, we calculated $R_s(P)$ at each of the temperatures for which we have data. The calculation follows that outlined in Sec. III, except that incompressibility is not assumed. The surface tension σ is used as a free parameter. The result yields values of R_s which fall within the domain of Eqs. (14) and (15), and those are used to fit the observed behavior of R_{eff} near melting at each temperature by choosing an appropriate value of σ. It was found, for example, that at 1.8 K, $\sigma = 0.043$ ergs/cm^2 and at 1.95 K, $\sigma = 0.105$ ergs/cm^2. We do not consider this outcome to be satisfactory. It was because we were disturbed that σ appeared to vary (less rapidly!) with temperature that the present measurements were undertaken in the first place.

To summarize this discussion, then, we have identified a possible qualitative explanation for why R_{eff} might decrease with increasing pressure under certain conditions, but the explanation does not give a satisfactory quantitative account of the observations, and we therefore do not believe it to be well established. In particular, if σ is approximately independent of temperature as one would expect, R_{eff} would not be expected to decrease (or remain constant) with increasing pressure just near melting at each of the temperatures studied as we have observed it to do. To study the question further will require measurements of η and μ over a larger portion of the P, T plane in order to determine whether R_{eff} at least behaves qualitatively as the appropriate hydrodynamic calculation predicts over a larger domain.

The questions that arise in connection with this work are important. Does an ion cause a solid sphere to condense about itself? This question may be related to the mechanism of nucleation of solidification of the bulk.[20] It is possible that further light may be thrown on it by studies of impurity ions in helium.[24] Can the behavior of ions be studied using continuum thermodynamics and hydrodynamics with bulk parameters? Can the otherwise inaccessible solid-liquid surface tension be deduced from the behavior of ions? Can we learn more about the properties of the supercooled liquid by studying ions? We think the present work has opened or reopened these questions in part due to the precision of the measurements, which has made possible comparisons which were not possible before.

ACKNOWLEDGMENTS

We are indebted to L. Bruschi and M. Santini for preparing the vibrating-wire viscometer module for us, to T. J. Sluckin for help in data reduction, to R. W. Zwanzig and J. Mathews for valuable theoretical insights concerning the hydrodynamic problem, and to L. Mori for technical assistance.

---

†Supported by the Italian agencies Consiglio Nazionale delle Ricerche and Comitato Nazionale per l'Energia Nucleare, and by NSF Grant No. DMR71-01819 under the U.S.-Italy joint cooperative research program.

*Permanent address: Laboratori Nazionali del Comitato Nazionale per l'Energia Nucleare Frascati, Roma, Italy.

‡Permanent address: California Institute of Technology, Low Temperature Physics 63-37, Pasadena, California 91125.

§Permanent address: Pennsylvania State University, Physics Dept., University Park, Penn. 16802.

[1]D. Goodstein, A. Savoia, and F. Scaramuzzi, Phys. Rev. A 9, 2151 (1974).
[2]L. Bruschi, G. Mazzi, M. Santini, and G. Torzo, J. Low Temp. Phys. 18, 487 (1975); R. Biskeborn and R. W. Guernsey, Jr., Phys. Rev. Lett. 34, 455 (1975).
[3]There is some overlap with the mobility data of B. Brody, Phys. Rev. B 11, 170 (1975).
[4]G. Ahlers and G. Gamota, Phys. Lett. A 28, 65 (1972).
[5]K. R. Atkins, Phys. Rev. 116, 1339 (1959).
[6]Precision pressure gauge, Model No. 145-01 produced by Texas Instruments.
[7]F. Scaramuzzi, Internal report LNF 63/79 CNEN-Roma (unpublished).
[8]In Ref. 1., Method C, p. 155.
[9]L. Bruschi and M. Santini, Rev. Sci. Instrum. 16, 1560 (1975).
[10]J. T. Tough, W. D. McCormick, and J. G. Dash, Rev. Sci. Instrum. 35, 1345 (1964).
[11]J. Goodwin, thesis (University of Washington, 1968) (unpublished).
[12]Data for the equation of state were taken from E. R. Grilly, Phys. Rev. 149, 97 (1966) and D. L. Elwell and H. Meyer, *ibid.* 164, 245 (1967).
[13]R. H. Romer, and R. J. Duffy, Phys. Rev. 186, 255 (1969).
[14]G. Ahlers, in *The Physics of Liquid and Solid Helium*, edited by K. H. Bennemann and J. B. Ketterson, (Wiley, New York, 1976).
[15]D. L. Goodstein, Phys. Rev. B 11, 5210 (1977).
[16]R. A. Ferrell, H. Menyhard, H. Schmidt, F. Schwabl, and P. Szepfalusy, Ann. Phys. (N.Y.) 47, 565 (1968).
[17]R. M. Ostemeier and K. W. Schwarz, Phys. Rev. A 5, 2510 (1972).
[18]A. Savoia, F. Scaramuzzi and D. L. Goodstein in *Low Temperature Physics-LT14*, edited by M. Krusius and M. Vuorio (North-Holland, Amsterdam, 1975).
[19]See also F. T. Bartis, Phys. Lett. A 60, 417 (1977).
[20]M. W. Cole and T. J. Sluckin, J. Chem. Phys. 67, 746 (1977). M. W. Cole and R. A. Bachman, Phys. Lett. A 58, 465 (1976); Phys. Rev. B 15, 1388 (1977).
[21]R. W. Zwanzig (private communication).
[22]L. D. Landau and E. M. Lifshitz, *Fluid Mechanics* (Pergamon, London, 1959), p. 54.
[23] L.D. Landau and E. M. Lifshitz, *Fluid Mechanics* (Pergamon, London, 1959), p. 65. The result remains valid to lowest order in $(R_0/R_s)^4$ if one includes deviations of the velocity field from the Stokes form. [J. Mathews (private communication).]
[24]M. W. Cole and F. Toigo (unpublished).